# Enhanced correlations and superconductivity in weakly interacting partially flat-band systems: A determinantal quantum Monte Carlo study

Edwin W. Huang,[1,2] Mohammad-Sadegh Vaezi,[3,4] Zohar Nussinov,[4] and Abolhassan Vaezi[1,5,*]

[1]*Department of Physics, Stanford University, Stanford, California 94305, USA*

[2]*Stanford Institute for Materials and Energy Sciences, SLAC National Accelerator Laboratory and Stanford University, Menlo Park, California 94025, USA*

[3]*Pasargad Institute for Advanced Innovative Solutions, Tehran 1991633361, Iran*

[4]*Department of Physics, Washington University, St. Louis, Missouri 63160, USA*

[5]*Stanford Center for Topological Quantum Physics, Stanford University, Stanford, California 94305, USA*

(Received 25 November 2018; revised manuscript received 8 April 2019; published 13 June 2019)

Motivated by recent experiments realizing correlated phenomena and superconductivity in two-dimensional (2D) van der Waals devices, we consider the general problem of whether correlation effects may be enhanced by modifying band structure while keeping a fixed weak interaction strength. Using determinantal quantum Monte Carlo, we study the 2D Hubbard model for two different band structures: a regular nearest-neighbor tight-binding model and a partially flat-band structure containing a nondispersing region, with identical total noninteracting bandwidth $W_{\rm tot}$. For both repulsive and attractive weak interactions ($|U| \ll W_{\rm tot}$), correlated phenomena are significantly stronger in the partially flat model. In the repulsive case, even with $U$ being an order of magnitude smaller than $W_{\rm tot}$, we find the presence of a Mott insulating state near half filling of the flat region in momentum space. In the attractive case, where generically the ground state is superconducting, the partially flat model exhibits significantly enhanced superconducting transition temperatures. These results suggest the possibility of engineering correlation effects in materials by tuning the noninteracting electronic dispersion.

DOI: 10.1103/PhysRevB.99.235128

## I. INTRODUCTION

The recent discovery of superconductivity in twisted bilayer graphene (TBG) [1,2] has spurred increasing interest in two-dimensional (2D) van der Waals materials with structural deformations [3–10] and has inspired new venues to search for high-$T_c$ superconductivity [11–18]. In TBG, the band structure hosts tiny regions near the $K$ and $K'$ valleys with nearly flat energy dispersions [19–24]. When these regions are partially occupied, a phase diagram similar to that of high-$T_c$ cuprates has been reported [1,2]. Alongside and possibly compounding other effects (e.g., [25]), it is widely believed that due to the large density of states (DOS) at the two tiny (nearly) flat regions, the system exhibits strong correlation physics [2,26–37]. Besides the specific case of TBG, a series of recent experiments has shown superconductivity in a variety of twisted heterostructures [38–41], supporting the generic possibility of achieving correlation effects by modifying band structure. Inspired by these experiments on moiré heterostructures and the broader quest of understanding flat bands [42–44], we introduce "partially flat-band" (PFB) models wherein the band structure is neither fully flat nor fully dispersive (see Fig. 1). In PFBs, the bare kinetic (i.e., not interaction induced [45,46]) dispersion $\epsilon_{\mathbf{k}}$ is nearly flat over a finite fraction of the Brillouin zone (BZ) with a diverging DOS.

There are no reliable theoretical tools to obtain the effective low-energy action for the PFB. Perturbation theory fails due to the divergence of the DOS over a finite portion of the BZ. Other conventional methods of strongly correlated systems such as the Wolff-Schrieffer transformation become inapplicable. These difficulties are tied to the existence of three significantly different energy scales: (i) the bandwidth associated with the flat region, (ii) the total bandwidth, and (iii) the interaction energy scale, which is much greater than (i) yet far smaller than (ii). Interactions can mix the smoothly connected flat and dispersive regions. These two regions may actively exchange particles and energy. Thus, if the nearly flat region is partially filled, the dispersive region cannot be disregarded. A projection of the interactions onto the flat region is unjustified.

To better grasp the physics of PFB systems, we introduce a toy model allowing numerical studies on general lattices. Herein, a large fraction (of order 1) of the band structure is (nearly) flat. We utilize the determinental quantum Monte Carlo (DQMC) approach to obtain the phase diagram for both repulsive and attractive weak Hubbard interactions. Due to the existence of flat areas, correlation effects are pronounced, and we expect to encounter evidence of strong-correlation physics despite only weak interactions. In particular, we observe an emergent Mott insulating state near *half filling* of the *flat region* in momentum space. Our calculations show that the momentum space electron occupation number becomes nearly uniform and fractional all over the flat region. This is inconsistent with the Luttinger theorem and constitutes another indication that we either have a gapless non-Fermi liquid or a Mott insulating phase. Last, we find a considerable enhancement of the superconducting transition temperature for attractive

*vaezi@stanford.edu

 

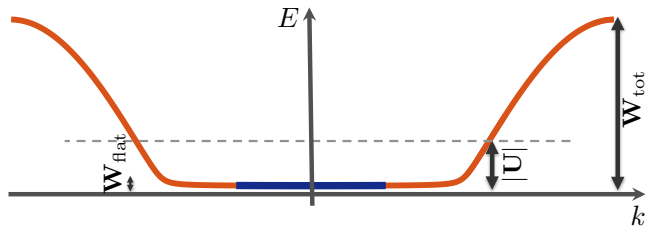


FIG. 1. A schematic band structure of partially flat-band systems. The band structure contains a (nearly) flat region with a high DOS and a narrow bandwidth $W_{\text{flat}}$. In the PFB system, the interaction energy scale may be much smaller (larger) than the total (flat-region) bandwidth; thus, $W_{\text{flat}} \ll |U| \ll W_{\text{tot}}$. The blue region denotes occupied energy states when the interaction is switched off. However, using DQMC, we find that all single-particle states inside the flat region are (almost) equally occupied upon considering interaction effects (see the text). Due to the absence of any mass gap between the flat and dispersive areas, the two regions are strongly coupled through interactions.

interactions which can be generated via, e.g., retarded phonon-mediated electron-electron coupling [31,47–49].

## II. MODEL

The Hubbard model Hamiltonian is given by

$$H = \sum_{\mathbf{k}\sigma} \epsilon_{\mathbf{k}} c^{\dagger}_{\mathbf{k}\sigma} c_{\mathbf{k}\sigma} + U \sum_{i} n_{i\uparrow} n_{i\downarrow}. \tag{1}$$

Here, $c^{\dagger}_{\mathbf{k}\sigma}$ creates an electron of momentum $\mathbf{k}$ and spin $\sigma$, the (noninteracting) band dispersion is $\epsilon_{\mathbf{k}}$, and $n_{i\sigma} = c^{\dagger}_{i\sigma} c_{i\sigma}$ is the number operator on site $i$. The local (on-site) interaction is parameterized by $U$. Thanks to its possible relevance to high-$T_c$ cuprate superconductors, the repulsive ($U > 0$) Hubbard model on a square lattice has been the focus of many numerical studies [50–52]. Due to the fermion sign problem in quantum Monte Carlo (QMC) simulations of the repulsive Hubbard model, unbiased numerical results are absent at temperatures relevant to the putative superconducting phase of the model (although a variety of techniques suggest the presence of $d$-wave superconductivity and various competing phases [53–57]). By contrast, the attractive Hubbard model ($U < 0$) is amenable to sign-problem-free QMC simulations, allowing for detailed characterization of the $s$-wave superconducting phase, including calculation of $T_c$. We will study both the repulsive and attractive realizations of this model.

For simplicity and to ease comparison to existing studies of Hubbard models, we performed the simulations on the commonly studied periodic square-lattice geometries. Here, the band structure

$$\epsilon_{\mathbf{k}} = \left[1 + f \,\mathrm{sgn}\left(\epsilon^0_{\mathbf{k}}\right)\right] \epsilon^0_{\mathbf{k}}, \tag{2}$$

where the nearest-neighbor-hopping dispersion $\epsilon^0_{\mathbf{k}} = -2t\,(\cos k_x + \cos k_y)$ and the parameter $f$ controls the flatness of the band. The nearest-neighbor hopping $t$ is set to 1 as the unit of energy and temperature in this work. For $f = 1$, the dispersion $\epsilon_{\mathbf{k}} = 0$ when $\epsilon^0_{\mathbf{k}} \leqslant 0$ (half the BZ), and $\epsilon_{\mathbf{k}} = 2\epsilon^0_{\mathbf{k}}$ otherwise. We refer to the $f = 0$ model as the "regular-band" Hubbard model and to the $f = 1$ system as the "PFB Hubbard model."

Importantly, the total bandwidth is fixed to $W_{\text{tot}} = 8$ in either case. Hence, our data showcase the effects of introducing a flat region in the noninteracting dispersion while keeping the total bandwidth constant. We focus on the hole-doped models (average occupancy $\langle n \rangle = \langle n_\uparrow + n_\downarrow \rangle < 1$), such that if $f = 1$, the noninteracting Fermi level lies inside the flat region.

## III. REPULSIVE INTERACTION

We first consider the repulsive model with a partially flat band and weak interactions $U \leqslant 2$. The presence of the fermion sign problem restricts accessible temperatures to $T \gtrsim U/15$ for moderate system sizes (∼100 sites), with certain fillings amenable to somewhat lower temperatures. Interestingly, the average sign in the DQMC simulation is enhanced near a density of $\langle n \rangle \sim 0.6$ per unit cell and decreases rapidly away from this value [Fig. 2(a)]. This behavior is reminiscent of that in the repulsive Hubbard model with a regular band, where the sign is protected by particle-hole symmetry at exactly half filling ($\langle n \rangle = 1$); doping away from half filling

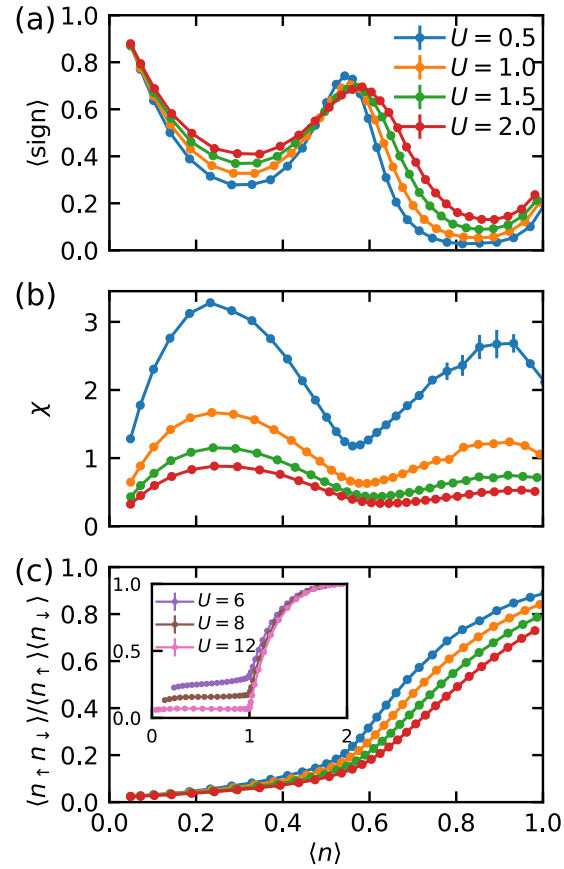


FIG. 2. Doping dependence of (a) average fermion sign, (b) charge compressibility $\chi = \frac{\partial \langle n \rangle}{\partial \mu}$, and (c) double-occupancy ratio in the partially flat-band model with a repulsive interaction $U > 0$. In the inset of (c), we plot the double-occupancy ratio for the regular-band Hubbard model with strong interactions. Simulations here are on a $16 \times 8$ periodic cluster at temperature $T = U/15$. Error bars are $\pm 1$ standard error of the mean, determined by jackknife resampling.

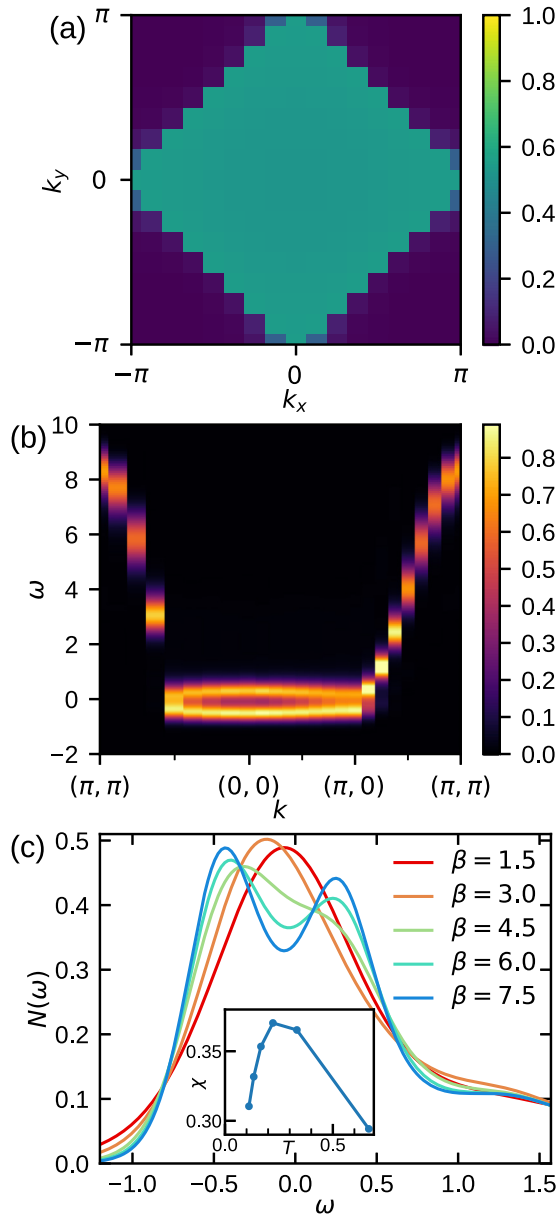


FIG. 3. (a) Momentum-resolved electron filling $\langle n_{\mathbf{k}}\rangle = \langle c^{\dagger}_{\mathbf{k}} c_{\mathbf{k}}\rangle$ for the partially flat-band model with repulsive interaction $U = 2$ at temperature $T = 0.133$ and average filling $\langle n\rangle = 0.62$ on a periodic $16 \times 16$ cluster. (b) Single-particle spectral function $A(\mathbf{k}, \omega)$ along high-symmetry cuts obtained for the same simulation using maximum entropy analytic continuation. (c) Single-particle density of states $N(\omega)$ for the same parameters at inverse temperatures $\beta = 1/T$ as given in the legend. Inset: Charge compressibility as a function of temperature.

(such that $\langle n\rangle \neq 1$) leads to a severe sign problem [58,59]. While no such symmetry is exactly manifest in the partially flat model, the similar behavior of the $\langle n\rangle \sim 0.6$ PFB system to the regular Hubbard model at half filling hints at similar (Mott insulating) underlying physics.

To confirm this, we examine the charge compressibility $\chi = \frac{\partial\langle n\rangle}{\partial\mu}$ in Fig. 2(b). As a function of filling, $\chi$ has a pronounced dip around $\langle n\rangle \sim 0.6$. The compressibility at $\langle n\rangle = 0.62$ decreases with lowering temperature [Fig. 3(c), inset], indicating insulating behavior and suggesting an incompressible gapped ground state. To relate this behavior to Mott physics and quantitatively assess correlation effects, we compare the number of doubly occupied sites $\langle n_{\uparrow} n_{\downarrow}\rangle$ to the uncorrelated case (in which $\langle n_{\uparrow} n_{\downarrow}\rangle = \langle n_{\uparrow}\rangle\langle n_{\downarrow}\rangle = \langle n\rangle^2/4$). The ensuing ratio is plotted in Fig. 2(c). For a regular Hubbard model [inset of Fig. 2(c)], at half filling, this ratio is suppressed when there are strong interactions. This ratio remains suppressed upon hole doping but rises for electron doping where double occupancy becomes unavoidable. In the PFB model, we observe the same behavior relative to a filling of $\langle n\rangle \sim 0.6$, at which a crossover occurs. The suppression, even for $U \sim 1$, of double occupancy in the PFB system is comparable in magnitude to that of the regular-band Hubbard model with $U \sim 8$. Taken together, the analogies between the weakly interacting PFB model and the regular-band strongly interacting Hubbard model demonstrate that even weak interactions can enable correlated phenomena given the correct band structure.

Having established a Mott insulating state in the PFB model when $\langle n\rangle \sim 0.6$, we now explore in greater depth the momentum and energy dependence of the single-particle properties. In Fig. 3(a), we plot the electron occupancy $\langle n_{\mathbf{k}}\rangle = \langle c^{\dagger}_{\mathbf{k}} c_{\mathbf{k}}\rangle$. As is evident from Eq. (2), the nondispersive flat region is delineated by $|k_x| + |k_y| \leqslant \pi$. In this region, the electron occupancy varies from 0.52 to 0.55, while the total filling [Fig. 3(a)] is $\langle n\rangle = 0.62$. Thus, the crossover seen in Fig. 2 at $\langle n\rangle \sim 0.6$ corresponds to a half filling of the flat portion of the PFB. Inconsistency with Luttinger's theorem implies a gapless non-Fermi-liquid-type behavior or a featureless gapped (Mott insulating) state, and considering other evidence we presented earlier, we believe it should be a Mott insulator. This special behavior of the occupancy suggests a modified mean-field approach to the PFB for the effective low-energy action from which the emergence of the Mott insulator becomes obvious (see the Appendix).

To corroborate these statements, we computed the single-particle spectral function $A(\mathbf{k}, \omega)$ by an analytical continuation of the imaginary-time Green's function using the maximum entropy method [60]. Figure 3(b) shows $A(\mathbf{k}, \omega)$ along high-symmetry cuts of the BZ. The most pertinent feature is the presence of a Mott gap throughout the flat region. In Fig. 3(b), for $U = 2$ and a temperature $T = 0.133$, the gap is largest ($\sim$0.8) at $\mathbf{k} = (0, 0)$ and gradually drops near the boundaries of the flat region. Figure 3(c) provides the single-particle density of states $N(\omega) = \frac{1}{L^2}\sum_{\mathbf{k}} A(\mathbf{k}, \omega)$ for different temperatures; the gap opening temperature is estimated to be between $T = 0.22$ and 0.33 concomitant with the onset of insulating behavior in the charge compressibility (inset).

## IV. ATTRACTIVE INTERACTION

While we have found strong indications of Mott insulating physics in the repulsive partially filled model with only weak interactions, the sign problem prevents a detailed study of phases that emerge by doping away from $\langle n\rangle \sim 0.6$. By contrast, we can establish concrete results on the effect of the modified band structure on superconductivity in the attractive Hubbard model via DQMC [61]. In 2D simulations, accurate estimates of superconducting $T_c$

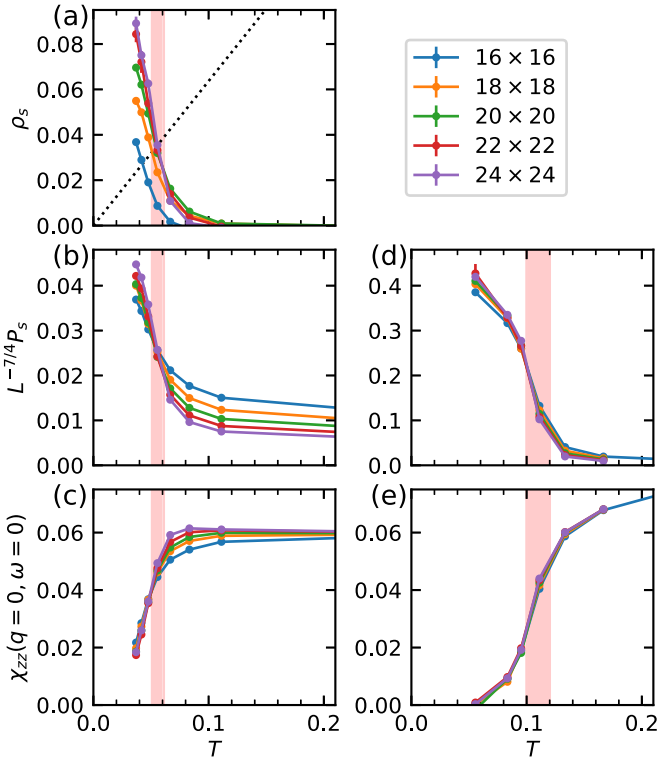


FIG. 4. Estimates of the superconducting transition temperature $T_c$ for (a)–(c) the regular attractive and (d) and (e) PFB Hubbard models. Here, $U = -2$, and $\langle n \rangle = 0.8$. We plot the superfluid stiffness $\rho_s$ in (a), the $s$-wave pair-field susceptibility multiplied by $L^{-7/4}$ in (b) and (d), and the static spin susceptibility in (c) and (e). The dashed line in (a) is $2T/\pi$. The shaded regions indicate estimates of $T_c$.

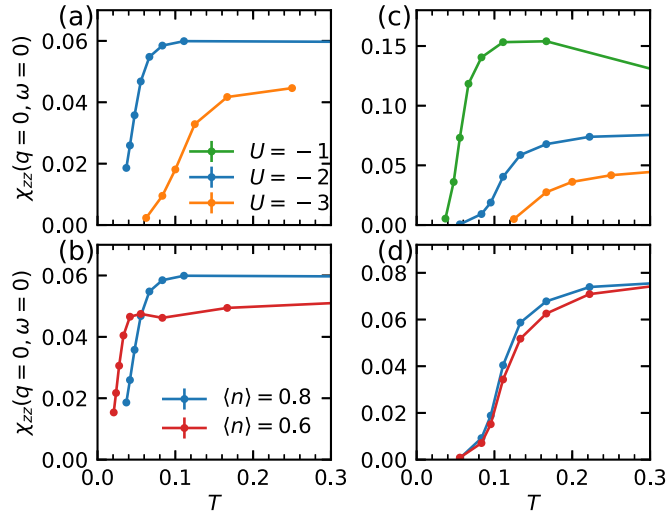


FIG. 5. Parameter dependence of static spin susceptibility (a) and (b) in the regular attractive Hubbard model and (c) and (d) in the partially flat band model. The downturn in the static spin susceptibility signals formation of singlet pairs and provides a rough indication of $T_c$.

may be obtained using the Nelson-Kosterlitz criterion for superfluid stiffness: $\rho_s(T_c) = 2T_c/\pi$. For finite-cluster simulations, the temperature where $\rho_s(T)$ intersects with $2T/\pi$ estimates $T_c$ in the thermodynamic limit. In DQMC, $\rho_s$ may be calculated as [62] $\rho_s = \frac{1}{4}[\Lambda_{xx}(q_x \to 0, q_y = 0) - \Lambda_{xx}(q_x = 0, q_y \to 0)]$, where the static current-current susceptibility $\Lambda_{xx}(\mathbf{q}) = \sum_i \int_0^\beta d\tau\, e^{-i\mathbf{q}\cdot\mathbf{r}_i} \langle j_x(i,\tau) j_x(0,0)\rangle$. Here, the current density operator $\mathbf{j}(i) = \sum_{l\sigma} it_{il}(\mathbf{r}_i - \mathbf{r}_l) c^\dagger_{i\sigma} c_{l\sigma}$, where $t_{il}$ is the hopping (related to the dispersion through $t_{il} = -\frac{1}{L^2}\sum_{\mathbf{k}} e^{i\mathbf{k}\cdot(\mathbf{r}_i - \mathbf{r}_l)}\epsilon_{\mathbf{k}}$.)

We show the results of this analysis in Fig. 4(a) for the attractive regular-band Hubbard model for $U = -2$ and $\langle n \rangle = 0.8$. Comparing simulations on different cluster sizes allows us to estimate $T_c \approx 0.056(5)$ for these parameters. Here, the minimal cluster size for a reasonable estimate of $T_c$ is $\sim 20 \times 20$. (In a previous DQMC simulation of the attractive Hubbard model [62] for $U = -4$, a lattice of size $\sim 10 \times 10$ was sufficient for estimating $T_c$. For low $|U|$, the longer superconducting coherence length requires larger clusters to mitigate finite-size effects.)

A PFB requires many real-space hopping amplitudes to be nonzero. Consequently, the computation of the current correlator becomes expensive. As an alternative, we infer $T_c$ from the behavior of the pair field susceptibility and of the static spin susceptibility. The equal-time $s$-wave pair field susceptibility is given by $P_s = \langle\{\Delta, \Delta^\dagger\}\rangle$, where $\Delta^\dagger = \frac{1}{L}\sum_i c^\dagger_{i\uparrow} c^\dagger_{i\downarrow} = \frac{1}{L}\sum_{\mathbf{k}} c^\dagger_{\mathbf{k}\uparrow} c^\dagger_{-\mathbf{k}\downarrow}$ is the $s$-wave pair field creation operator at zero net momentum. The spin susceptibility is given by $\chi_{zz}(\mathbf{q},\tau) = \langle T_\tau S_z(\mathbf{q},\tau) S_z^\dagger(\mathbf{q})\rangle$, where $S_z(\mathbf{q}) = \frac{1}{L}\sum_i e^{-i\mathbf{q}\cdot\mathbf{r}_i}(c^\dagger_{i\uparrow} c_{i\uparrow} - c^\dagger_{i\downarrow} c_{i\downarrow})$. We focus on the static spin susceptibility at $\mathbf{q} = 0$: $\chi_{zz}(\mathbf{q}, \omega = 0) = \int_0^\beta d\tau\, \chi_{zz}(\mathbf{q},\tau)$. (We consider only the $z$ component of spin; $\chi_{xx}$, $\chi_{yy}$, and $\chi_{zz}$ are identical within statistical errors).

Upon cooling below $T_c$, one expects that the formation of singlet pairs suppresses the static spin susceptibility. In the absence of a pseudogap, the onset temperature of this suppression provides an estimate of $T_c$. A corresponding rise of the pair field susceptibility would confirm that the suppression of spin susceptibility is due to the onset of superconductivity.

Figures 4(a)–4(e) display the results of DQMC calculations for the temperature dependence of the pair field susceptibility and the static spin susceptibility. For the regular band, we observe the expected downturn in spin susceptibility and rise in pair field susceptibility near $T_c \approx 0.056(5)$. Similar behavior occurs in the PFB model at $T_c \approx 0.11(1)$ (in the PFB model, the system size dependence is weak, but it is computationally infeasible to simulate even larger clusters to eliminate the possibility of a gradual shift). Together these data indicate that the attractive Hubbard model with a PFB has doubled the superconducting transition temperature of the model with a regular dispersion. This increase is partially anticipated by the larger density of states in the PFB. We emphasize that this is while keeping the interaction strength and the total noninteracting bandwidth fixed.

An enhancement of superconductivity in the attractive PFB appears for different interaction strengths and dopings. In Figs. 5(a) and 5(b), we vary the interaction strength for both the regular band and the PFB models. As before, the downturn in the static spin susceptibility roughly indicates $T_c$. When $|U| = 3$, the Hubbard model $T_c$ rises to 0.12(2) for

the regular band model and 0.18(2) for the PFB model. For a smaller interaction strength of $|U| = 1$, the PFB model has $T_c \approx 0.06(5)$, while the $T_c$ of the regular band model was too low to be readily accessible. In Figs. 5(c) and 5(d), we contrast the effects of additional hole doping within the two models. As the number density varies from $\langle n\rangle = 0.8$ to $\langle n\rangle = 0.6$, the regular-band Hubbard model $T_c$ decreases from 0.056(5) to 0.035(5), while the PFB model shows little variation in its $T_c$.

## V. CONCLUSIONS

We introduced and studied PFB systems. PFBs may be realized in diverse experimental arenas, e.g., TBG or heavy-fermion systems. Our DQMC analysis illustrated that the existence of flat subregions enhances the correlation effects even for interactions significantly weaker than the total bandwidth. We found a Mott insulating state for weak local repulsion and an $s$-wave superconductor with a considerably enhanced $T_c$ for weak local attraction. Our PFB model may aid the understanding of TBG and other Moiré heterostructures whose band structure hosts extremely tiny (nearly) flat areas due to the very large spatial extent of the moiré superlattices. Studying systems with such supercells is not computationally feasible. As we discussed earlier, the dispersive nonflat regions that are connected to small, flat domains of the TBG may not be ignored. Thus, a projection of the Hamiltonian onto the flat region is not possible. One needs to keep single-particle (hole) excitations with energies of the order of the interaction scale $|U|$ above (below) the flat region. Our PFB model captures these essential features and provides a simple toy model to study TBG which is computationally feasible as well (albeit by imposing triangular-lattice symmetry).

The ideal PFB (i.e., the model exhibiting exactly flat subregions of the band) requires the existence of finite hopping amplitudes between distant sites. Nonetheless, we may truncate these amplitudes beyond a cutoff distance without impacting the low-energy physics. In doing so, we may still achieve nearly flat regions with enhanced correlation. Remarkably, augmenting a nearest-neighbor-hopping tight-binding amplitude ($t = 1$) by an additional next-nearest-neighbor-hopping amplitude $t_2 \approx -0.54$ suffices to achieve a high DOS in the lower half of the band structure on the square lattice. Such a simple model might be realizable in 2D van der Waals devices with square-lattice symmetry or in cold-atom systems via photoinduced coupling experiments or through applying pressure and is expected to have an amplified superconducting transition temperature.

## ACKNOWLEDGMENTS

We acknowledge helpful discussions with H. Aoki, S. Sayyad, and H. Jiang. E.W.H. was supported by the U.S. Department of Energy (DOE), Office of Basic Energy Sciences, Division of Materials Sciences and Engineering, under Contract No. DE-AC02-76SF00515. Computational work was performed on the Sherlock cluster at Stanford University. M.-S.V. and Z.N. acknowledge partial support from the National Science Foundation (Grant No. NSF 1411229). M.S.V. also acknowledges the financial support from Pasargad Institute for Advanced Innovative Solutions under the Supporting Grant scheme (Project No. SG1-RCM1810-01).

## APPENDIX: A MODIFIED MEAN-FIELD APPROACH TO THE PARTIALLY FLAT-BAND SYSTEMS

In this Appendix, we discuss a modified mean-field theory that can successfully explain quintessential features of PFB systems, e.g., the emergence of the Mott insulator near the half filling of the flat region. The essential ingredient is the fact that the occupation number of the single-particle energy eigenstates does not follow the Fermi-Dirac distribution since we have a Fermi volume rather than a Fermi surface. Instead, the $k$-space occupancy is uniform over the flat region (where the chemical potential crosses). Thus, all associated flat-band states are partially occupied.

Motivated by the physics of the square-lattice regular Hubbard model near half filling, we focus on the antiferromagnetic order. We assume that $\langle \frac{n_{i,\uparrow}-n_{i,\downarrow}}{2}\rangle = (-1)^i m$, where $m$ denotes the staggered magnetization. We invoke the standard mean-field approximation $n_{i,\uparrow}n_{i,\downarrow} \approx \langle n_{i,\uparrow}\rangle n_{i,\downarrow} + n_{i,\uparrow}\langle n_{i,\downarrow}\rangle - \langle n_{i,\uparrow}\rangle\langle n_{i,\downarrow}\rangle$. Plugging this approximation into the model Hamiltonian, Eq. (1) of the main text, and performing a Fourier transformation, we obtain

$$H_{\mathrm{MF}} = \sum_{k,\sigma}[(\epsilon_k - \mu)c^\dagger_{k,\sigma}c_{k,\sigma} - mU\sigma c^\dagger_{k+Q,\sigma}c_{k,\sigma} + \mathrm{H.c.}], \tag{A1}$$

where $Q = (\pi, \pi)$. The above mean-field Hamiltonian can be readily diagonalized. We then have

$$H_{\mathrm{MF}} = \sum_{|k_x|+|k_y|\leqslant\pi,\sigma} (E_{+,k}\gamma^\dagger_{+,k}\gamma_{+,k} + E_{-,k}\gamma^\dagger_{-,k,\sigma}\gamma_{-,k,\sigma}), \tag{A2}$$

where $E_{\tau,k} = \tau\sqrt{\epsilon_k^2 + (Um)^2} - \mu$ denotes the energy eigenvalue associated with band $\tau = \pm$ at momentum $k$ and $\gamma_{\tau,k}$ is the corresponding annihilation operator, which is a linear combination of $c_{k,\sigma}$ and $c_{k+Q,\sigma}$. The self-consistency of our assumption about the staggered magnetization implies the following identity:

$$m = \sum_i \frac{(-1)^i}{2N_s}\langle n_{i,\uparrow} - n_{i,\downarrow}\rangle_{H_{\mathrm{MF}}} = -mU\sum_{k,\tau}\frac{f(E_{\tau,k})}{E_{\tau,k}}. \tag{A3}$$

Here, $f(E_{\tau,k})$ denotes the occupation number of energy band $\tau$ at momentum $k$, and $N_s = L^2$ is the number of sites. Normally, $f$ is replaced by the Fermi-Dirac distribution, so that all negative-energy states (those below the chemical potential) are fully occupied at $T = 0$, and excited states (those above the chemical potential) are empty. In PFBs, the chemical potential crosses many zero-energy states (more than the total electron density), and thus, it is not, *a priori*, clear which states are occupied or empty. This feature can generally lead to exotic behaviors in flat-band systems such as the fractional quantum Hall systems. However, our DQMC study of the PFB system shows that the occupation number is nearly uniform all over the flat subregion where the chemical potential is tuned. We have verified that this remains the case even for nearly flat subregions (as long as the interaction scale is larger than the bandwidth $W_{\mathrm{flat}}$ of the subregion with a high DOS; see

Fig. 1 of the main text). Implementing this observation into the $f(E_{\tau,k})$ functional, we observe that, different from the regular-band Hubbard model, the mean-field antiferromagnetic order parameter remains finite even away from half filling (with the filling fraction being relative to that of the total band).

In the conventional-band Hubbard model, the Fermi-Dirac distribution can rationalize the appearance of antiferromagnetic order at half filling. However, at the mean-field level, any doping away from half filling (relative to the entire band structure), even if infinitesimal, will eradicate the antiferromagnetic order. Using the modified mean-field approximation, we find that although the flat subregion is partially occupied, the staggered magnetization is nonzero. Consequently, the antiferromagnetic spin-density wave (SDW) will open up a mass gap separating the (nearly) flat subregion from the dispersive subregions. In other words, an interaction-induced SDW mass gap will appear at the $|k_x| + |k_y| \leqslant \pi$ surface corresponding to half filling. Thanks to the existence of a finite gap separating the modified (nearly) flat region from the remaining band structure, we can focus on the lower flat subband and employ the standard techniques of the strongly correlated system on a modified (nearly) flat subband. One consequence of this simple analysis is that the system will exhibit a Mott insulating phase at half filling of the lower (nearly) flat emergent subband (i.e., at a quarter filling of the original band).

To summarize, the interaction generates an SDW order and doubles the unit cell, and the relevant flat subband around the chemical potential becomes separated from other bands (which were otherwise smoothly connected to the flat subband in the absence of interaction). Note that the bandwidth and structure factors of the emergent (nearly) flat subband differ from those of the original flat subregion. The emergent well-separated (nearly) flat subband is not fully occupied, and the interaction-projected emergent flat subband will dictate its fate. Mott physics, as well as other related strong-correlation phenomena, is possible. This picture can easily be generalized to more complicated situations where the (nearly) flat subregion is smaller by considering smaller nesting vectors (different and shorter $Q$ vectors) that lead to larger unit cells.


[1] Y. Cao, V. Fatemi, S. Fang, K. Watanabe, T. Taniguchi, E. Kaxiras, and P. Jarillo-Herrero, Nature (London) **556**, 43 (2018).

[2] Y. Cao, V. Fatemi, A. Demir, S. Fang, S. L. Tomarken, J. Y. Luo, J. D. Sanchez-Yamagishi, K. Watanabe, T. Taniguchi, E. Kaxiras, R. C. Ashoori, and P. Jarillo-Herrero, Nature (London) **556**, 80 (2018).

[3] K. S. Novoselov, A. K. Geim, S. Morozov, D. Jiang, M. Katsnelson, I. Grigorieva, S. Dubonos, and A. A. Firsov, Nature (London) **438**, 197 (2005).

[4] Y. Zhang, Y.-W. Tan, H. L. Stormer, and P. Kim, Nature (London) **438**, 201 (2005).

[5] F. Guinea, M. Katsnelson, and A. Geim, Nat. Phys. **6**, 30 (2010).

[6] L. Ju, Z. Shi, N. Nair, Y. Lv, C. Jin, J. Velasco Jr., C. Ojeda-Aristizabal, H. A. Bechtel, M. C. Martin, A. Zettl, J. Analytis, and F. Wang, Nature (London) **520**, 650 (2015).

[7] A. Vaezi, Y. Liang, D. H. Ngai, L. Yang, and E.-A. Kim, Phys. Rev. X **3**, 021018 (2013).

[8] F. Zhang, A. H. MacDonald, and E. J. Mele, Proc. Natl. Acad. Sci. USA **110**, 10546 (2013).

[9] I. Martin, Y. M. Blanter, and A. F. Morpurgo, Phys. Rev. Lett. **100**, 036804 (2008).

[10] Q. H. Wang, K. Kalantar-Zadeh, A. Kis, J. N. Coleman, and M. S. Strano, Nat. Nanotechnol. **7**, 699 (2012).

[11] J. G. Bednorz and K. A. Müller, Z. Phys. B **64**, 189 (1986).

[12] M. K. Wu, J. R. Ashburn, C. J. Torng, P. H. Hor, R. L. Meng, L. Gao, Z. J. Huang, Y. Q. Wang, and C. W. Chu, Phys. Rev. Lett. **58**, 908 (1987).

[13] P. W. Anderson, Science **235**, 1196 (1987).

[14] E. Fradkin, S. A. Kivelson, and J. M. Tranquada, Rev. Mod. Phys. **87**, 457 (2015).

[15] P. A. Lee, N. Nagaosa, and X.-G. Wen, Rev. Mod. Phys. **78**, 17 (2006).

[16] K. Kuroki, S. Onari, R. Arita, H. Usui, Y. Tanaka, H. Kontani, and H. Aoki, Phys. Rev. Lett. **101**, 087004 (2008).

[17] I. I. Mazin, D. J. Singh, M. D. Johannes, and M. H. Du, Phys. Rev. Lett. **101**, 057003 (2008).

[18] Y. Kamihara, T. Watanabe, M. Hirano, and H. Hosono, J. Am. Chem. Soc. **130**, 3296 (2008).

[19] E. Suárez Morell, J. D. Correa, P. Vargas, M. Pacheco, and Z. Barticevic, Phys. Rev. B **82**, 121407(R) (2010).

[20] R. Bistritzer and A. H. MacDonald, Proc. Natl. Acad. Sci. USA **108**, 12233 (2011).

[21] E. J. Mele, Phys. Rev. B **81**, 161405(R) (2010).

[22] G. Trambly de Laissardiere, D. Mayou, and L. Magaud, Nano Lett. **10**, 804 (2010).

[23] S. Fang and E. Kaxiras, Phys. Rev. B **93**, 235153 (2016).

[24] L. Zhang, Science Bulletin **64**, 495 (2019).

[25] B. Padhi, C. Setty, and P. W. Phillips, Nano Lett. **18**, 6175 (2018).

[26] T. T. Heikkilä and G. E. Volovik, in *Basic Physics of Functionalized Graphite* (Springer, Cham, 2016), pp. 123–143.

[27] G. E. Volovik, JETP Lett. **107**, 516 (2018).

[28] F. Wu, T. Lovorn, E. Tutuc, and A. H. MacDonald, Phys. Rev. Lett. **121**, 026402 (2018).

[29] N. F. Q. Yuan and L. Fu, Phys. Rev. B **98**, 045103 (2018).

[30] H. C. Po, L. Zou, A. Vishwanath, and T. Senthil, Phys. Rev. X **8**, 031089 (2018).

[31] J. F. Dodaro, S. A. Kivelson, Y. Schattner, X. Q. Sun, and C. Wang, Phys. Rev. B **98**, 075154 (2018).

[32] B. Roy and V. Juričić, Phys. Rev. B **99**, 121407(R) (2019).

[33] L. Rademaker and P. Mellado, Phys. Rev. B **98**, 235158 (2018).

[34] X. Y. Xu, K. T. Law, and P. A. Lee, Phys. Rev. B **98**, 121406(R) (2018).

[35] C. Xu and L. Balents, Phys. Rev. Lett. **121**, 087001 (2018).

[36] H. Guo, X. Zhu, S. Feng, and R. T. Scalettar, Phys. Rev. B **97**, 235453 (2018).

[37] N. F. Q. Yuan, H. Isobe, and L. Fu, arXiv:1901.05432.

[38] G. Chen, A. L. Sharpe, P. Gallagher, I. T. Rosen, E. Fox, L. Jiang, B. Lyu, H. Li, K. Watanabe, T. Taniguchi, J. Jung, Z. Shi, D. Goldhaber-Gordon, Y. Zhang, and F. Wang, arXiv:1901.04621.

[39] S. Moriyama, Y. Morita, K. Komatsu, K. Endo, T. Iwasaki, S. Nakaharai, Y. Noguchi, Y. Wakayama, E. Watanabe, D. Tsuya, K. Watanabe, and T. Taniguchi, arXiv:1901.09356.
[40] C. Shen, N. Li, S. Wang, Y. Zhao, J. Tang, J. Liu, J. Tian, Y. Chu, K. Watanabe, T. Taniguchi, R. Yang, Z. Y. Meng, D. Shi, and G. Zhang, arXiv:1903.06952.
[41] X. Liu, Z. Hao, E. Khalaf, J. Y. Lee, K. Watanabe, T. Taniguchi, A. Vishwanath, and P. Kim, arXiv:1903.08130.
[42] V. I. Iglovikov, F. Hébert, B. Grémaud, G. G. Batrouni, and R. T. Scalettar, Phys. Rev. B **90**, 094506 (2014).
[43] R. Ojajärvi, T. Hyart, M. A. Silaev, and T. T. Heikkilä, Phys. Rev. B **98**, 054515 (2018).
[44] R. Mondaini, G. G. Batrouni, and B. Grémaud, Phys. Rev. B **98**, 155142 (2018).
[45] V. A. Khodel, J. W. Clark, and M. V. Zverev, Phys. Rev. B **78**, 075120 (2008).
[46] V. R. Shaginyan, V. A. Stephanovich, A. Z. Msezane, P. Schuck, J. W. Clark, M. Y. Amusia, G. S. Japaridze, K. G. Popov, and E. V. Kirichenko, J. Low Temp. Phys. **189**, 410 (2017).
[47] T. J. Peltonen, R. Ojajärvi, and T. T. Heikkilä, Phys. Rev. B **98**, 220504(R) (2018).
[48] F. Wu, A. H. MacDonald, and I. Martin, Phys. Rev. Lett. **121**, 257001 (2018).
[49] B. Lian, Z. Wang, and B. A. Bernevig, arXiv:1807.04382.
[50] D. J. Scalapino, Rev. Mod. Phys. **84**, 1383 (2012).
[51] T. Maier, M. Jarrell, T. Pruschke, and M. H. Hettler, Rev. Mod. Phys. **77**, 1027 (2005).
[52] J. P. F. LeBlanc, A. E. Antipov, F. Becca, I. W. Bulik, G. K.-L. Chan, C.-M. Chung, Y. Deng, M. Ferrero, T. M. Henderson, C. A. Jiménez-Hoyos, E. Kozik, X.-W. Liu, A. J. Millis, N. V. Prokof'ev, M. Qin, G. E. Scuseria, H. Shi, B. V. Svistunov, L. F. Tocchio, I. S. Tupitsyn, S. R. White, S. Zhang, B.-X. Zheng, Z. Zhu, and E. Gull (Simons Collaboration on the Many-Electron Problem), Phys. Rev. X **5**, 041041 (2015).
[53] T. A. Maier, M. Jarrell, T. C. Schulthess, P. R. C. Kent, and J. B. White, Phys. Rev. Lett. **95**, 237001 (2005).
[54] P. Corboz, T. M. Rice, and M. Troyer, Phys. Rev. Lett. **113**, 046402 (2014).
[55] B.-X. Zheng, C.-M. Chung, P. Corboz, G. Ehlers, M.-P. Qin, R. M. Noack, H. Shi, S. R. White, S. Zhang, and G. K.-L. Chan, Science **358**, 1155 (2017).
[56] E. W. Huang, C. B. Mendl, H.-C. Jiang, B. Moritz, and T. P. Devereaux, npj Quantum Mater. **3**, 22 (2018).
[57] H.-C. Jiang and T. P. Devereaux, arXiv:1806.01465.
[58] E. Y. Loh, J. E. Gubernatis, R. T. Scalettar, S. R. White, D. J. Scalapino, and R. L. Sugar, Phys. Rev. B **41**, 9301 (1990).
[59] V. I. Iglovikov, E. Khatami, and R. T. Scalettar, Phys. Rev. B **92**, 045110 (2015).
[60] M. Jarrell and J. E. Gubernatis, Phys. Rep. **269**, 133 (1996).
[61] R. Blankenbecler, D. J. Scalapino, and R. L. Sugar, Phys. Rev. D **24**, 2278 (1981).
[62] T. Paiva, R. R. dos Santos, R. T. Scalettar, and P. J. H. Denteneer, Phys. Rev. B **69**, 184501 (2004).